

Lawrence Berkeley National Laboratory

LBL Publications

Title

Vertical movement of soluble carbon and nutrients from biocrusts to subsurface mineral soils

Permalink

<https://escholarship.org/uc/item/7pk678v4>

Authors

Young, Kristina E
Ferrenberg, Scott
Reibold, Robin
et al.

Publication Date

2022

DOI

10.1016/j.geoderma.2021.115495

Copyright Information

This work is made available under the terms of a Creative Commons Attribution-NonCommercial License, available at <https://creativecommons.org/licenses/by-nc/4.0/>

Peer reviewed

1 Vertical movement of soluble carbon and nutrients from biocrusts to subsurface mineral soils

2

3 Kristina E. Young^{1*}, Scott Ferrenberg², Robin Reibold³, Sasha C. Reed³, Tami Swenson⁴, Trent

4 Northen^{4,5}, Anthony Darrouzet-Nardi¹

5 1. Biological Sciences, University of Texas at El Paso 500 W. University Ave. University of

6 Texas at El Paso, El Paso, TX 79968

7 2. Department of Biology New Mexico State University, Foster Hall, 1305 Frenger St, Las

8 Cruces, NM 88001

9 3. U.S. Geological Survey, Southwest Biological Science Center, 2290 S. West Resource

10 Blvd. Moab, UT 84532

11 4. Environmental Genomics and Systems Biology Division, Lawrence Berkeley National

12 Laboratory, 1 Cyclotron Road, Berkeley, CA 94720

13 5. DOE Joint Genome Institute, 2800 Mitchell Dr., Walnut Creek, CA, 94598, USA

14 * corresponding author: keyoung1@miners.utep.edu

15

16 Keywords: cryptogam, desert, nutrient cycling, soil fertility, biogeochemistry, metabolite

17

18 **Abstract**

19

20 Dryland ecosystems can be constrained by low soil fertility. Within drylands, the soil
21 nutrient and organic carbon (C) cycling that does occur is often mediated by soil surface
22 communities known as biological soil crusts (biocrusts), which cycle C and nutrients in the top
23 ca. 0 – 2 cm of soil. However, the degree to which biocrusts are influencing soil fertility and
24 biogeochemical cycling in deeper, subsurface mineral soils is unclear. The movement of
25 dissolved resources from biocrusts to deeper soil layers in leachate may be one of the main
26 mechanisms through which biocrust fertility is transferred downward towards deeper microbial
27 communities and plant roots occurring within mineral soil. Here we examined the role of
28 biocrust leachate in contributing to subsurface nutrient and soluble C pools and subsurface
29 microbial cycling. We collected biocrusts from three biocrust successional stages and explored
30 resource pools *in situ* at multiple soil depths, while collecting leachate and measuring nutrient
31 and organic C concentrations and metabolite composition from each successional stage in the
32 laboratory. After four leachate collections, we conducted an incubation of mineral soil collected
33 from below each biocrust successional stage to measure heterotrophic microbial CO₂ flux and
34 biomass. Overall, our findings observed that the degree of nutrient and C connectivity between
35 biocrusts and the sub-crust mineral soil depended on the biocrust successional stage and the
36 element being considered, and the influence of biocrust successional stage on mineral soil CO₂
37 flux is likely related to long-term resource build up. Together, our results suggest that the
38 influence of biocrust leachate on subsurface mineral soil is complex and context dependent, but,
39 over longer time periods and at later successional stages, can have measurable effects on dryland
40 soil biogeochemical cycling with feedbacks to resource availability and CO₂ flux.

41

42 **1. Introduction**

43 Within drylands, productivity and function can be co-limited by water, nutrients, and
44 carbon (C) (Austin, 2011). Understanding the pathways through which nutrients and C enter and
45 are retained within dryland soils is therefore essential for understanding ecosystem processes in
46 this expansive biome (Hartley et al., 2007; Rudgers et al., 2018). Yet, we have a limited
47 understanding of how common soil surface communities in drylands, known as biological soil
48 crusts (biocrusts), are biogeochemically connected with the mineral soil below (deeper than 2
49 cm) (Barger et al., 2016). Biocrusts contain varying levels of lichens, mosses, cyanobacteria,
50 fungi, algae, and other macro- and micro- organisms often occurring in successional stages
51 (Belnap & Lange 2001). These biocrusts can influence surface soil fertility through their roles as
52 soil stabilizers (Chaudhary et al., 2009), CO₂-fixers (Wertin et al. 2012; Darrouzet-Nardi et al.,
53 2015; Sancho et al., 2016), contributors of nitrogen (N) via N₂ fixation (Barger et al., 2016;
54 Torres-Cruz et al., 2018), and regulators of soil microbial communities (Baran et al., 2015), in
55 addition to contributing to plant nutrients, as shown through isotopic labeling (Mayland and
56 McIntosh, 1966; Stewart, 1967). Contributions from biocrust have the capacity to be particularly
57 significant in ecosystems notable for their low soil organic matter reservoirs and overall low
58 levels of soil fertility (Collins et al., 2014).

59 One mechanism through which nutrients and C move from biocrusts into the mineral soil
60 is downward transport during and following pulsed precipitation events (Barger et al., 2016).
61 Water leached through the biocrust layer can carry with it ammonium (NH₄⁺) and nitrate (NO₃⁻)
62 biogenic phosphorus (P) and a wide variety of metabolites (Barr, 1999; Johnson et al., 2005;
63 Porada et al., 2014; Baran et al., 2015; Swenson et al., 2018). However, studies of the chemical
64 makeup and the fate of biocrust-sourced dissolved compounds are rare and contradictions exist

65 within the literature as to biocrusts' contribution to subsurface soil nutrients and organic matter.
66 In some cases, biocrusts have been shown to increase the levels of subsurface nutrients and
67 organic C, such as inorganic N (Guo et al., 2008; Barger et al., 2016; Chamizo et al., 2012;
68 Ferrenberg et al., 2018), while in others, some subsurface nutrients and organic C were similar
69 beneath biocrusts types, plants, and bare ground (Delgado-Baquerizo et al., 2013; Moreira-Grez
70 et al., 2019). Further, biocrust communities are comprised of different morphological groups and
71 species, which can differ across desert and soil types (Colesie et al., 2016) and along
72 successional gradients within a given area (Housman et al., 2006), with consequences for the
73 amounts and forms of compounds leached into subsurface soil (Johnson et al., 2005; Tucker et
74 al., 2020).

75 Biocrust-derived leachate may also influence subsurface microbial communities, with
76 implications for nutrient retention and gaseous release from mineral soil layers, as seen with leaf
77 litter in other ecosystems (e.g., Cleveland et al., 2010). Exudates from biocrust can structure soil
78 microbial communities and soil food webs adjacent to biocrusts (Baran et al., 2015). However,
79 the extent to which leachate influences deeper soil microbial communities is unclear. Microbial
80 operational taxonomic units (OTUs) below biocrusts can be similar across different biocrust and
81 soil types (Moreira-Grez et al., 2019; Steven et al., 2013), with the notable exception of moss
82 crust, which can have higher microbial biomass and community diversity in the mineral soil
83 below the moss compared to earlier successional, cyanobacteria-dominated biocrust stages (Bao
84 et al., 2019; Delgado-Baquerizo et al., 2015) possibly due to the large amounts of organic C
85 released from moss crusts, which can structure microbial communities (Baran et al. 2015). The
86 variability in resource inputs from different biocrust types and differences in the microbial
87 communities below biocrust types underscore the likelihood of varying levels of connectivity

88 between the biocrust layer and the mineral soil below. Connectivity between the biocrust and the
89 microbial communities and functions in the mineral soil layer has implications for microbial
90 nutrient turnover, resource storage, and CO₂ respiration in both the short and long term
91 (Cleveland et al., 2010).

92 Here, we present a novel experimental design that sought to assess biocrusts'
93 connectivity with mineral soil using multiple successional stages of biocrust. Specifically, we
94 examined lightly pigmented, darkly pigmented, and moss dominated biocrust that represent a
95 generalized gradient of succession in our study system from least to most developed (Belnap et
96 al. 2001, Belnap & Eldridge 2001). Lightly pigmented cyanobacterial crusts are early colonizers
97 and are generally dominated by the cyanobacterial *Microcoleus spp.* (Rosentreter & Belnap
98 2001, Couradeau et al., 2016). Darkly pigmented crusts, generally dominated *Microcoleus spp.*
99 and *Scytonema spp.*, (Rosentreter & Belnap 2001, Couradeau et al., 2016) and moss dominated
100 crusts are considered more developed, later successional forms of biocrust. Darkly pigmented
101 cyanobacteria crusts generally have high rates of N fixation, while darkly pigmented and moss
102 crusts have high rates of C fixation when compared to lightly pigmented crusts (Housman et al.
103 2006; Tucker et al. 2019). For this experiment, we located an area with a relatively homogenous
104 sandy soil type and assessed the differences in connectivity among the three biocrust
105 successional stages and the mineral soil below. We addressed the following questions: (1) What
106 compounds are leached from the biocrust layer during wet-up events and do the compounds
107 differ among biocrust types? and (2) Do compounds leached from the different biocrust
108 successional stages regulate short-term microbial activity in sub-surface soils? In addressing
109 these two questions, this experiment lends insight into the role of dissolved resources moving
110 from biocrusts into the mineral soil and the short-term consequences of these inputs for

111 heterotrophic respiration, with implications for a larger understanding of nutrient and C cycling
112 in dryland soils.

113 114 **2. Material and Methods**

115
116 This study consisted of three complementary components that each assessed soil or
117 leachate associated with different biocrust successional states on the Colorado Plateau, USA.
118 These three components consisted of a field assessment of nutrient and C concentrations in *in-*
119 *situ* biocrust and the below-biocrust mineral soil, a laboratory assessment of potential leachate
120 chemistry, and a soil incubation with biocrust leachate. Biocrust types consisted of an early
121 successional, lightly pigmented cyanobacterial biocrust (i.e., likely dominated by *Microcoleus*
122 *vaginatus*, (Rosentreter & Belnap 2001, Garcia-Pichel et al. 2013)), a mid-successional darkly
123 pigmented cyanobacterial biocrust (likely dominated by *Microcoleus vaginatus* and *Scytonema*
124 spp., (Rosentreter & Belnap 2001, Couradeau et al., 2016)), and a mid to late successional moss
125 dominated biocrust (dominated by *Syntrichia caninervis*, Weber et al., 2016). Biocrust samples
126 were collected in January 2017 in a 25 m² area of semiarid desert outside of Moab, UT (38°41'
127 02.31" N, 109°43' 11.60" W, 1,529 m above sea level). The soil type was visually homogenous,
128 with the soils characterized as a well-drained, fine sandy loam on average 86 cm deep in the
129 Begay-Sazi-Rizo complex (Soil Survey Staff, NRCS). Inorganic C varied from 0.16% to 0.67%
130 in the crust layer and 0.07% to 0.97 % in the mineral soil layer (Supplemental Table 1). Soils in
131 the region are generally neutral to alkaline, pH ranged from 7.26-7.84 in the biocrust layer and
132 7.67-8 in the mineral subsoil (Supplemental Table 1). The ecological site was a Four-Wing
133 Saltbush semidesert with a mean annual precipitation of 30 cm and a mean annual temperature of
134 10 °C. Parent material was alluvium and eolian deposits derived from sandstone (Soil Survey
135 Staff, NRCS). The three different successional stages were co-occurring within the 25 m² area.

136 The co-occurrence of different biocrust successional stages was likely due to past physical
137 disturbance, potentially the historic presence of cattle, which disturb biocrusts in discrete patches
138 and can leave other patches intact. However, the site was visually undisturbed during biocrust
139 collection.

140 *2.1 Assessment of biocrust and mineral soil in the field*

141 To determine the *in-situ* C and nutrient concentrations both within and below the different
142 biocrust types, we collected biocrust samples using a 10 x10 cm metal square core down to 2 cm
143 depth. A flat metal sheet was slid under the square core to remove the biocrust ($n = 10$ for each
144 crust type). On the exposed soil in the 10 x 10 cm area, we took three 2.54 cm diameter cores of
145 8 cm length (2-10 cm below crust surface), which were combined into one sample ($n = 10$ for
146 each crust type). We sieved the soil through a 4 mm sieve, removed roots and visible organic
147 matter, and homogenized before subsampling for extractions.

148 To determine total C and N concentrations, we dried a subset of each sample at 60 °C,
149 ground the samples, and measured for total C and N on an elemental analyzer (Elementar Vario
150 Micro Cube, Elementar Inc., Langenelsbold, Germany). Many dryland soils contain carbonates;
151 thus, determining total organic C concentrations from total C value requires assessment or
152 removal of inorganic C. Soil inorganic C concentrations were measured using a modified
153 pressure calcimetry assay (Sherrod et al. 2002). Briefly, a homogenized soil sample was sealed
154 in a 20 mL amber jar and exposed to hydrochloric acid in excess. A pressure transducer was then
155 used to measure the pressure from the resultant CO₂. Organic C was then calculated as total C
156 with inorganic C subtracted. To determine the pigment concentrations of lightly and darkly
157 pigmented biocrust samples, we extracted chlorophyll *a* (Chl_a) and scytonemin (Scy) with 90 %
158 acetone for 12 hours in the dark at 4 °C after being finely ground (Castle et al., 2011). The

159 supernatant was decanted, and pigment concentrations were measured spectrophotometrically
160 (GENESYS 10S UV-VIS, Thermo Scientific, Waltham, MA) at 665 nm and 394 nm for Chl_a and
161 Scy, respectively. The equation to convert the A₆₆₅ value to [Chl_a] was taken from Ritchie 2008
162 and conversion of the A₃₉₄ values to [Scy] was performed as in Garcia-Pichel and Castenholz
163 (1991). We measured organic matter concentrations of the lightly pigmented, darkly pigmented,
164 and moss biocrusts by loss-on-ignition of an oven-dried (105 °C) sample in a muffle furnace at
165 550 °C for 4 hr ((Davies, 1974); ThermoScientific Thermolyne, Waltham, MA, USA).

166 We extracted inorganic N pools, NH₄⁺ and NO₃⁻, using 2 M KCl and fresh soil. The soil
167 slurry was shaken for 1 hour then allowed to settle overnight (Robertson et al., 1999). Inorganic
168 N concentrations (NH₄⁺ and NO₃⁻) were quantified colorimetrically using the indophenol blue
169 method for NH₄⁺ and using a Cd-column reduction followed by the Greiss-Ilosvay method for
170 NO₃⁻ on a Smartchem 200 Discrete Autoanalyzer (Unity Scientific, Milford, MA). Soil PO₄³⁻ was
171 extracted using Olsen's method, with a 0.5 M NaHCO₃ solution and a shaking time of 16 hr
172 (Olsen, 1954). Soil extractable PO₄³⁻ and microbial PO₄³⁻ concentrations were quantified using a
173 modified ascorbic acid molybdate analysis (Kuo, 1996) on a Smartchem 200 Discrete
174 Autoanalyzer (Unity Scientific, Milford, MA). Limit of quantification was 0.02 mg PO₄³⁻-P/l for
175 all P measurements. Microbial C, N, and P concentrations were estimated with a chloroform cell
176 lysis method by adding 1 ml of amylene-stabilized CHCl₃ to soil in a 125 ml flask that was
177 stoppered with neoprene and allowed to sit in the dark for 16 hr before being ventilated and
178 extracted with 0.5 M K₂SO₄ (for microbial biomass C and N, Beck et al., 1997; Brookes et al.,
179 1985) or 0.5 M NaHCO₃ (for microbial biomass PO₄³⁻) and shaken for 1 hr (Weintraub et al.,
180 2007). Microbial biomass C, N, and P were calculated as the amount extracted from
181 nonfumigated soil subtracted from the amount extracted from fumigated soil. No microbial

182 biomass correction factors were applied (Weintraub et al., 2007). All extracts were filtered
183 through Whatman #1 filter paper (GE Healthcare, Chicago, IL). Extractable organic C, total
184 dissolved N, and microbial biomass C and N were analyzed on a Shimadzu TOC-V_{CPN} with the
185 TNM-1 attachment (Shimadzu Corporation, Kyoto, Japan). Determining the concentrations of
186 the biomass, nutrient, and C concentrations both within and below biocrusts provides a point-in-
187 time assessment of biologically available pools in the field.

188 *2.2. Assessment of leachate chemistry*

189 On the same day and at the same site as the collections described above, we collected intact
190 cores of each biocrust successional state ($n = 15$ for each stage), 2 cm deep and 4.6 cm in
191 diameter. We returned the cores to the laboratory and used them to determine the nutrient
192 concentrations of potential leachate from different biocrust successional states over a four-week
193 period. Once in the lab, we used a razor blade to carefully scrape the subsoil from the biocrust.
194 The subsoil could be differentiated from the biocrust layer by the lack of cohesion between soil
195 particles and the lack of visible cyanobacterial filaments or rhizomes. Because the crust layer
196 varies in thickness, specifically between successional stages, the biocrust thickness was different
197 for each sample and ranged from 6 mm – 12 mm for lightly and darkly pigment cyanobacterial
198 crusts and 10 mm – 15 mm for moss (Supplemental Table 1). We seated the cores in plastic
199 cylinders that were open on the top and had mesh screen on the bottom. Below the mesh screen
200 was a second cylinder with a layer of marbles resting on top of a second layer of mesh screen.
201 The marbles were to ensure sediment did not pool on the bottom of the mesh, to control the flow
202 of leachate during extractions, and to improve connectivity for liquid movement between the
203 mesh layers (Figure 1).

204 Once a week for four weeks, we added 30 ml of deionized water to lightly pigmented and
205 darkly pigmented crusts, 35 ml of deionized water to moss crusts, and 25 ml to blank controls
206 that did not have any biocrust but maintained all other aspects of the infrastructure. These
207 volumes corresponded to 15-21 mm of rainfall and were chosen to ensure enough liquid moved
208 through the sample and was available for C and nutrient analyses. Differences in watering
209 amount were accounted for in the final $\mu\text{g/ml}$ calculations. After allowing the liquid to saturate
210 the biocrust and move downward with gravity for 10 minutes, we placed the biocrust cores onto
211 a vacuum filtration system to pull remaining liquid through the biocrust system and we collected
212 the liquid in vials below the samples. We analyzed the collected liquid leachate for NH_4^+ , NO_3^- ,
213 PO_4^{3-} , extractable organic C and total dissolved N as described above. The concentrations in the
214 leachate were summed across the four time points to compare across biocrust types. To examine
215 differences in the nutrients within leachate and the nutrients with the soil crust layer between
216 biocrust types, we standardized nutrients “lost” in leachate to those occurring in the biocrust
217 layer using the equation: $((\text{sum nutrient leached})/(\text{nutrient amount in biocrust})) \times 100$

218 To assess metabolites in the leachate, we combined leachate from each sample across the
219 four-time points of the experiment and then compiled three replicates from the same biocrust
220 type together into one sample, so that the total number for each biocrust type was $n = 3$. We did
221 this to ensure we had enough sample to perform the analysis. The relative concentrations of key
222 metabolites were profiled using normal phase liquid chromatography (Merck SeQuant ZIC-
223 HILIC column, 150_1 mm, 3.5 mm, 100 Å) coupled to an Agilent 6520 ESI-Q-TOF at the
224 Lawrence Berkeley National Laboratory (Sparks et al., 1996). For metabolomics, approximately
225 30 ml liquid leachate were lyophilized (FreeZone 2.5 Plus, Labconco) and resuspended in 200 μl
226 methanol containing internal standards (5-50 μM of ^{13}C - ^{15}N Cell Free Amino Acid Mixture,

227 Sigma). Samples were vortexed for 20 seconds, filtered through 0.2 μm centrifugal filters and
228 placed into LC-MS vials for analysis. LC-MS data were acquired using an Agilent 1290 LC
229 stack with a HILIC column (Merck SeQuant ZIC-HILIC column, 150_1 mm, 3.5 mm, 100 \AA)
230 coupled to a Q Exactive Orbitrap MS (Thermo Scientific). Metabolites were identified using the
231 Metabolite Atlas and verified based on exact mass and retention time (< 1 min difference) and
232 MS/MS fragmentation spectra matching to known standards (Supplemental Table 2 &
233 Supplemental Table 3). Differences between relative amounts of metabolites were determined by
234 normalizing the peak area for each metabolite to the high peak value across biocrust types.

235

236 *2.3 Assessment of CO₂ flux and microbial biomass after leachate addition*

237 To answer our question exploring the relationship between leachate and heterotrophic
238 microbial activity, we conducted a soil incubation experiment where we added leachate from
239 each biocrust successional stage (collection described in 2.2. above) to the mineral soil collected
240 from beneath biocrusts in a full-factorial design. Specifically, mineral soil samples from the
241 same site described above were collected in July 2019 from beneath lightly pigmented
242 cyanobacterial, darkly pigmented cyanobacterial, and moss dominated biocrusts and soils were
243 given leachate collected from each of the crust types ($n = 3$ for each below-crust soil–leachate
244 pairing). We collected mineral soil by removing the 0-2 cm layer of lightly pigmented, darkly
245 pigmented, and moss-dominated biocrusts using a 10 x 10 cm square core and collected soil
246 beneath by taking 3, 4.6 cm diameter cores at a depth of 2-5 cm. For our incubation, we added
247 15 g of the below-biocrust mineral soil to 120 ml gas-tight glass Mason jars fitted with rubber
248 septa and brought the soil to 50 % of water holding capacity (around 2 ml per sample) with
249 leachate. We sealed the jar for 24 hours in the dark and then used a syringe to mix and collect 8

250 ml of headspace without exposing the headspace to the atmosphere. We analyzed CO₂
251 concentration of the headspace using a benchtop infrared gas analyzer (IRGA; CA-10, Sable
252 Systems International, North Las Vegas, NV). Soil respiration rate was calculated as μmol CO₂
253 g⁻¹ hr⁻¹. Before and after the 24-hr incubation we extracted the samples for microbial biomass C
254 concentration assessment as described above.

255 *2.4 Statistics*

256 We checked the data for normality and homogeneity of variance and found that many of
257 the response variables were non-normal and heteroscedastic. We used permutational ANOVAs,
258 which do not assume data normality or homogeneous variance, to determine how strongly
259 response variables differed across biocrust successional states. We conducted a pairwise
260 permutational test to determine how different the response variables were from one another
261 among the biocrust successional states. The permutational ANOVAs were conducted using the
262 package ‘VEGAN’ in R (Oksanen et al., 2019) and the permutational pairwise test was
263 conducted using the package ‘pairwiseAdonis’ in R (Arbizu, 2017). We also calculated the
264 differences in the magnitudes among the crust types for each response variable. The differences
265 in magnitude are reported as ratios such as $\bar{X}_{light}:\bar{X}_{dark}$ where \bar{X}_{light} is the mean of the lightly
266 pigmented cyanobacterial biocrusts for a given variable and \bar{X}_{dark} is the mean of the darkly
267 pigmented cyanobacterial biocrust for the same variable. The data were non-negative, showed
268 some degree of log normality and contained zeroes. As such, we calculated 95 % confidence
269 intervals for the ratios using a maximum-likelihood method designed for data with these features
270 (Zhou and Tu, 2000). Confidence intervals not containing 1 are considered statistically
271 significant for $H_0 = 1$, which would correspond to a 1:1 ratio, or no difference among crust types
272 (likelihood ratio test; Zho and Tu, 1999; Zhou and Tu, 2000). The calculations were conducted

273 using the package ‘treteffect’ in R (Darrouzet-Nardi, 2020). To compare relative intensify of
274 detected metabolites, we created a heat map using the function “heatmap.2” in the package
275 “gplots v3.1.1” in R and the hierarchical clustering with the package used the complete argument
276 in the “hclust” function (Figure 3). A two-way ANOVA and Tukey HSD test at an alpha level of
277 < 0.05 was used to indicate the normalized metabolite amounts that differed significantly among
278 biocrust types.

279

280 **3. Results**

281 *3.1 Characterization of biocrust successional states*

282 The Chl_a and Scy concentrations were higher in darkly pigmented cyanobacterial, mid-
283 successional biocrusts than in the early successional lightly pigmented cyanobacterial biocrusts
284 (Figure 2, Supplemental Table 4). Chlorophyll *a* concentrations were 5.5 times [4.11, 7.45; 95 %
285 CI] as high in darkly pigmented as in lightly pigmented cyanobacterial crusts ($p = 0.001$, $F =$
286 143.84). Scytonemin concentrations were 9.8 times [6.24, 15.5; 95 % CI] as high in darkly
287 pigmented as in lightly pigmented cyanobacterial crusts ($p = 0.001$, $F = 90.70$). The percent
288 organic matter increased across biocrust successional states ($p = 0.001$, $F = 59.78$), increasing 2.3
289 times [1.87, 2.67; 95 % CI] from lightly pigmented biocrust to darkly pigmented cyanobacterial
290 crust ($p < 0.001$), and then 1.8 times [1.52, 2.34, 95 % CI] from darkly pigmented cyanobacterial
291 to moss dominated biocrust ($p < 0.001$).

292

293 *3.2 Nutrients and organic C*

294 *3.2.1 N concentrations*

295 Generally, N concentrations in the biocrust layer were higher within darkly pigmented
296 cyanobacterial and moss biocrusts than in lightly pigmented cyanobacterial crusts (Figure 3 A.,
297 B., C., Supplemental Table 4). For example, total soil N and extractable NH_4^+ concentrations
298 were around twice as high in darkly pigmented cyanobacteria and moss dominated biocrusts than
299 lightly pigmented cyanobacterial crusts (NH_4^+ dark:light = 2.6 [1.99, 3.42; 95 % CI], moss:light
300 = 2.8 [1.91, 4.45; 95 % CI]) (% Total N dark:light = 1.92 [1.56, 2.37; 95 % CI], moss:light = 2.26
301 [1.73, 2.93; 95 % CI]). Extractable NO_3^- concentrations were the exception, with NO_3^- values
302 highest in the darkly pigmented cyanobacterial crust but similarly low in the other two crust
303 types ($p = 0.011$, $F = 3.61$). The ratio of organic C to total N was 1.4 times [1.23, 1.67; 95% CI]
304 higher in moss crusts than in the lightly pigmented cyanobacterial crusts and 1.2 times [1.1,
305 1.44; 95% CI] higher in darkly pigmented crusts than in lightly pigmented crusts (Supplemental
306 Table 4).

307 For the leachate, total dissolved N concentration was highest in lightly pigmented
308 cyanobacterial crusts compared to moss or darkly pigmented cyanobacterial biocrusts, with the
309 latter having the lowest N concentration overall. For example, total dissolved N was 2.34 times
310 [1.34, 3.92; 95% CI] higher in leachate from the lightly pigmented cyanobacterial crusts as it was
311 from darkly pigmented cyanobacterial crusts ($p = 0.02$), while NO_3^- concentrations were 3.98
312 times [2.27, 6.97; 95 % CI] higher in lightly pigmented cyanobacterial biocrusts as it was in
313 moss crusts ($p < 0.001$). When comparing the N leached from the biocrust to the N found in the
314 biocrust layer, lightly pigmented cyanobacterial crusts lost more NH_4^+ (13.04%) and NO_3^-
315 (55.25%) relative to the amount within the biocrust layer, than either the moss ($\text{NH}_4^+ = 3.54$,
316 $\text{NO}_3^- = 8.74$) or darkly pigmented cyanobacterial crust ($\text{NH}_4^+ = 1.77$, $\text{NO}_3^- = 9.02$). The ratio of
317 extractable total dissolved organic C to total dissolved N in leachate grew substantially larger

318 along the successional gradient, with the C:N ratio 4.3 times [3.56, 5.31; 95% CI] greater in
319 leachate from mosses than leachate from lightly pigment cyanobacterial crusts and 1.7 times
320 [1.09, 2.73; 95% CI] greater than leachate from darkly pigment cyanobacterial crusts
321 (Supplemental Table 4).

322 There were few generalizable patterns for N forms within the mineral soil beneath the
323 biocrust, and the overall patterns of N concentrations in the soil layer did not reflect those in the
324 biocrust layer or its leachate. The largest differences were seen in the extractable NO_3^- and total
325 dissolved N concentrations in the soil, which were lower beneath lightly pigmented
326 cyanobacterial crusts compared to below darkly pigmented and moss crusts. Extractable NH_4^+
327 concentrations in the soil were 1.5 [1.08, 2.15; 95 % CI] times higher below lightly pigmented
328 crusts and 2.2 [1.56, 3.04, 95 % CI] times higher below moss crusts than below darkly
329 pigmented cyanobacterial crusts (Figure 3C).

330

331 *3.2.2 P concentrations*

332 The extractable PO_4^{3-} concentrations in the biocrust layer increased from lightly
333 pigmented to darkly pigmented cyanobacterial to moss crusts ($p = 0.002$, $F = 10.16$) (Figure 3D).
334 The PO_4^{3-} in the leachate had a similar pattern to extractable PO_4^{3-} in the biocrust layer, but the
335 variation among the biocrust successional states was larger ($p = 0.16$, $F = 1.99$) (Figure 3E). The
336 PO_4^{3-} concentrations in the soil layer below the biocrusts were about 1.5 times lower below
337 darkly pigmented cyanobacterial crust compared with the other two crust successional states
338 ([light:dark 1.4 [1.02, 1.79; 95% CI], moss:dark 1.62 [1.29, 2.03; 95% CI]), while microbial
339 biomass PO_4^{3-} concentrations were similar in soils below all three crust successional states ($p =$
340 0.53 , $F = 0.94$) (Figure 3F).

341

342 3.2.3 C concentrations

343 Extractable total dissolved organic C in the biocrust layer increased from lightly
344 pigmented to darkly pigmented cyanobacterial to moss crusts ($p = 0.004$, $F = 6.49$) (Figure 3G).
345 Dissolved organic C in the leachate from moss crusts was 2.5 times [1.7, 3.87; 95% CI] higher
346 than lightly pigmented crusts and 4 times [3.01, 5.54; 95% CI] higher than darkly pigmented
347 cyanobacterial crusts (Figure 3H). In the mineral soil below the biocrust, extractable total
348 dissolved organic C and microbial biomass C were much higher below moss crusts than below
349 lightly and darkly pigmented cyanobacterial crusts. For example, total dissolved organic C was
350 11.6 times [5.14, 26.37; 95% CI] higher in moss than in lightly pigmented cyanobacterial crusts.
351 Soil total organic C was similar between moss crusts and darkly pigmented cyanobacterial crusts
352 ($p = 0.07$) but was 2.47 [1.59, 3.82; 95% CI] times higher in moss crusts than in lightly-
353 pigmented crusts and 1.22 times [0.97, 1.55; 95% CI] higher in darkly-pigmented crusts than
354 lightly pigmented crusts (Figure 3I).

355

356 3.3 Metabolites in leachate

357 The LC-MS analysis showed a wide range of metabolites in the leachate from each
358 biocrust successional state. Most of the metabolites were verified with authentic standards, and
359 those that were not were considered putative and not included in the list of present metabolites.
360 Moss dominated crusts seemed to have the highest relative abundance of metabolites compared
361 to lightly and darkly pigment crusts. Hierarchical clustering grouped lightly pigmented and
362 darkly pigmented crusts together, separate from moss dominated crusts. Some, but not all,
363 metabolites differed strongly among biocrust successional stage (Figure 4, Supplemental Table

364 5). Many present metabolites were osmolytes (Figure 5). Of the five commonly recognized
365 osmolytes found with the leachate (ectoine, proline, betaine, choline, and trigonelline) only the
366 relative abundance of betaine and choline differed strongly among successional stages. Betaine:
367 moss:dark 3.49 [1.71, 7.12; 95% CI], moss:light 4.342 [1.13, 16.68; 95% CI], dark:light 1.24
368 [0.27, 5.7; 95% CI].

369

370 *3.4 Soil respiration and microbial C*

371 A full-factorial design crossing soils from beneath the different biocrusts with leachate
372 collected from the different biocrusts revealed that soil CO₂ respiration changed significantly as
373 a function of the successional state beneath which the mineral soils were collected ($p = 0.001$, F
374 $= 54.440$), but not as a function of the successional stage from where leachate was sourced ($p =$
375 0.452 , $F = 0.89$) (Figure 6, Supplemental Table 4). Because respiration rates did not differ
376 significantly among leachate sources on a given subsoil, we treated the four different leachates as
377 replicates when examining the relationship between CO₂ respiration and subsoils. Soil CO₂
378 respiration rates were similar in soils collected from beneath lightly pigmented and darkly
379 pigmented cyanobacterial crusts ($p = 0.92$) but were around 1.7 times higher in soils collected
380 from beneath moss biocrust (moss:light = 1.76 [1.52, 2.04; 95 % CI], moss:dark = 1.74
381 [1.56, 1.95; 95 % CI]; Figure 6). Microbial biomass C concentrations were also significantly
382 different across mineral soil types ($p = 0.001$, $F = 38.03$) but were similar among leachate
383 treatments ($p = 0.86$, $F = 0.24$). We again treated leachate types as replicates within mineral soil
384 types, since the differences among leachate types were small and not significant. Microbial
385 biomass C was around 2.3 times higher in mineral soil beneath darkly pigmented cyanobacterial
386 and moss crusts than below lightly pigmented crusts (dark:light = 2.28 [1.93, 2.7; 95 % CI],

387 moss:light = 2.31 [1.87, 2.85; 95% CI]). Mineral soil collected beneath lightly pigmented
388 cyanobacterial crust had the highest soil respiration to microbial biomass C ratio (activity :
389 biomass = 0.102) compared to darkly pigmented crust soil (activity : biomass = 0.045) and moss
390 crust soil (activity : biomass = 0.077). Note that the microbial biomass in the incubation
391 experiment were distinct from the *in-situ* microbial biomass measurements and not comparable
392 due to the differences in timing and method of collection.

393 394 **4. Discussion**

395 Here, we explored the connectivity between biocrusts and the subsurface mineral soil.
396
397 We found that biocrusts released a wide range of nutrients and organic C compounds during
398 leaching events and that the concentrations of C, N, and P in leachate differed widely among the
399 three biocrust successional stages, as did the degree to which the resources accumulated in the 2-
400 10 cm soil layer (Figure 3). Further, we found that leachate concentration did not appear to affect
401 short-term microbial heterotrophic CO₂ fluxes in mineral soil (Figure 6) as it has in other
402 ecosystem types (e.g., Cleveland et al., 2010). Instead, the provenance of mineral soil, with
403 regard to which biocrust successional state occurred on the surface where the soil was collected,
404 was the main driver of differences in CO₂ flux, suggesting a longer-term effect of biocrust type
405 on sub-surface microbial respiration. Overall, we observed that the degree of connectivity
406 between biocrusts and the mineral soil depends on the biocrust successional stage and the
407 resource being considered, and that changes to successional stage may have significant influence
408 on the biogeochemical connectivity between biocrusts and mineral soil.

409

410 *4.1 Nutrients and organic C in biocrust leachate*

411 The patterns in leached nutrients and C varied among biocrust type and element. For
412 example, lightly pigmented cyanobacterial crusts lost the most N in leachate of the three biocrust
413 types. This finding is surprising, given the dominant species of this area's lightly pigmented
414 crusts, *M. vaginatus*, is not a N-fixer; although, N fixation by free-living organisms tightly
415 associated with *M. vaginatus* is common, these rates are typically relatively low (Belnap, 2001;
416 Stegge et al., 1996). However, it's known that cyanobacteria secrete a large fraction of their
417 photosynthate into their surrounding environment (Baran et al., 2015; Thomazo et al., 2018), and
418 there is emerging evidence for a 'cyanosphere,' in which the pioneering soil cyanobacteria, *M.*
419 *vaginatus*, concentrates N-fixing bacteria around cyanobacterial bundles through organic C
420 exudation (Couradeau et al., 2019, Nelson et al. 2021). Our results build on these findings to
421 suggest the early-successional cyanosphere is less able to retain N than later-successional
422 cyanobacterial communities, and notably, that this cyanobacterial-dominated biocrust loses more
423 N relative to the N it stores in the biocrust layer. Similar patterns of N loss in leachate, including
424 large amounts of organic N loss, were observed in a separate experiment examining leached N
425 from lightly and darkly pigmented biocrusts collected on the Colorado Plateau (Johnson et al.,
426 2005). The ability of darkly pigmented crusts to retain more N and C than lightly pigmented
427 crusts suggests structural and/or species differences between lightly and darkly pigmented
428 biocrusts that allows microbial communities within darkly pigmented cyanobacterial biocrusts to
429 better retain resources. This could be related to the more complex species compositions that bind
430 and resorb nutrients (Garcia-Pichel et al., 2001; Garcia-Pichel and Belnap, 1996, Courdeau et al.
431 2019) and suggests another differences among the three biocrust types is the ability to retain
432 nutrients, specifically N. Our findings suggest lightly pigmented biocrusts maintain lower C and
433 nutrient stocks and are less able to maintain soil fertility in the 0-2 cm soil layer than later

434 successional crust types. But, surprisingly, may promote N fertility in deeper soil layers
435 disproportionate to their N stocks, as indicated by the larger amounts of N leached downward
436 from the surface.

437 The large stoichiometric differences in the leachate (for example, the large differences in
438 C:N between lightly and darkly pigmented cyanobacterial crust leachate) likely influences the
439 ultimate fate of the leachate, as well as the microbial communities that utilize and recycle it.
440 Nutrients and organic C in leachate may be resorbed, taken up by vascular plants, fungi, archaea,
441 or other bacteria, flushed to deeper soil layers, rapidly oxidized, or transformed and lost in
442 gaseous form (Barger et al., 2016), all of which could be influenced by changes in leachate
443 stoichiometry. Here, the dissolved C:N ratio in leachate doubled among successional stages,
444 suggesting that disproportionate amounts of dissolved organic C are being released into the soil
445 below late-successional crusts relative to N, likely structuring the complex communities found
446 there (Baran et al. 2015) but leading to a larger potential for N limitation in soils below late-
447 successional crusts. Because biocrust types are anticipated to change under global change
448 scenarios (Ferrenberg et al., 2015; Reed et al., 2016) understanding these stoichiometric
449 differences in biocrust leachate, as well as the connectivity among biocrust types and mineral
450 soil, is important for understanding the fate of these nutrients and C in transitioning drylands
451 (Ferrenberg et al., 2018b; Maestre et al., 2013; Reed et al., 2012). Further, changes in
452 precipitation patterns and increasing aridity will likely influence the degree of connectivity
453 between biocrust and the mineral soil. This is due to the predominant role of precipitation in
454 controlling the downward movement of water and therefore the degree to which the biocrust and
455 subsoil are connected (Collins et al. 2014). Less precipitation or smaller precipitation events may
456 decrease the degree to which biocrust contribute to subsoil nutrients.

457 The metabolite content in leachate also varied among biocrust successional stages. The
458 large amounts of organic C found in leachate from moss crusts is similar to other studies
459 examining biocrust leachate (Zhao et al., 2016) and contained a correspondingly large
460 concentration and diversity of metabolites. Osmolytes, specifically betaine, choline, ectoine,
461 trigonelline, and proline, were found in leachate from each biocrust type and most commonly in
462 moss crusts. There is evidence that these osmolytes are essential components of the desiccation
463 and rehydration of biocrusts (Swenson et al., 2015). The long list of other metabolites detected,
464 including amino acids, nucleotides, nucleobases, sugars, and vitamins, suggests additional
465 functions related to microbial activity. Metabolites are important components of microbial food
466 webs within biocrusts, with heterotrophs specializing in specific metabolites released from
467 cyanobacteria as substrates (Baran et al., 2015). The differences in metabolite content from
468 different biocrust types is likely related to the different complexities and structures within each
469 biocrust type. For example, extracellular polymeric matrixes (EPM) released as microbially-
470 produced exopolysaccharides from biocrusts can bind and capture metabolites, helping to retain
471 them in the biocrust layer (Swenson et al., 2018). Different amounts of EPM in the three crust
472 types (Rossi et al., 2018), as well as the large amounts of organic C derived from tissue and
473 rhizomes of moss crusts (Dümig et al., 2013), may help explain differences in leachate
474 metabolite content. Future work quantifying the various metabolites and directly comparing
475 concentrations of the observed metabolites with microbial activity would further our
476 understanding of these pools and their role in microbial activity in the soils below biocrust.

477

478 *4.2 Nutrient pools within and below biocrusts*

479 The nutrient and organic C concentrations of the 2-10 cm soil layer did not strongly
480 reflect the concentrations of the biocrust layer or the leachate, with the exceptions of moss crusts,
481 which leached large amounts of total dissolved organic C and had high total dissolved organic C
482 pools in the mineral soil (Figure 3). Some studies have observed a difference in nutrient and C
483 pools below biocrusts (Barger et al., 2013; Guo et al., 2008; Brankatschk et al., 2013) while
484 others have not (Beraldi-Campesi et al., 2009; Moreira-Grez et al., 2019; Yang et al., 2019)
485 reflecting a lack of consensus on the degree of connectivity between biocrusts and the mineral
486 soil below. This is not entirely surprising, as nutrient pools can change dramatically and
487 dynamically through time and, because they represent the net effect of multiple inputs and types
488 of uptake/loss (Hart et al., 1994), they may not correlate with inputs or be dissimilar across crust
489 types at a given time point. For example, in a separate experiment conducted on the Colorado
490 Plateau, soil NO₃⁻ concentrations in the 0-10 cm soil layer almost doubled between winter and
491 spring, while resin-extractable NO₃⁻ decreased around 17 times during the same time period
492 (Zelikova et al., 2012). A separate study measuring 0-5 cm below lightly pigmented and darkly
493 pigmented cyanobacterial crust on the Colorado Plateau did not observe large differences in
494 inorganic N amounts among crust types over time (Barger et al., 2005). To more fully explore
495 connectivity between biocrusts and the mineral soil, more studies examining resource pools
496 within the biocrusts and mineral soils across time are needed.

497

498 *4.3 Microbial CO₂ flux from sub-crust soils*

499 Nutrients leached from the different biocrust types did not change short-term
500 heterotrophic activity in sub-surface soils (Figure 6). This was unexpected, as we did see
501 significant differences in leachate chemistry across biocrust successional states (e.g., total

502 dissolved organic C concentrations were more than twice as high in leachate from late
503 successional moss dominated biocrust than in either of the earlier successional states) and as both
504 microbial respiration and biomass responded to differences in leachate concentrations in other
505 ecosystems (Cleveland et al., 2006; Qiu et al., 2005). While we observed short-term responses
506 here, it is possible we would see larger differences with longer incubation times. Soil respiration
507 rates in the mineral soil were relatively low compared with other systems, reinforcing the notion
508 that subsurface soils have lower microbial activity (Miralles et al., 2012). When looking at the
509 role of biocrust community type, the higher respiration rate coming from below the moss
510 biocrusts suggests a longer-term influence of crust leachate on sub-surface microbial activity.
511 The large amounts of organic C leached from moss crusts and the large total dissolved organic C
512 pools found in the mineral soil below moss crusts may serve as an easily accessible source of C
513 for heterotrophs in the mineral soil when water is available. These findings suggest a longer-term
514 influence of moss crust on the mineral soil and microbial cycling (Dümig et al., 2013), namely
515 through the accumulation of organic C in the soil over time, with consequences for the amount of
516 C being released from dryland soils.

517

518 **5. Conclusion**

519 The vertical movement of soluble C and nutrients from the biocrust layer to the mineral
520 soil may be one of the main mechanisms through which biocrusts contribute to mineral soil
521 fertility. Here, we observed that the degree of connectivity between biocrusts and the mineral soil
522 depends on the biocrust type and the resource being considered. The contrasting findings in the
523 literature as to the role biocrusts play in providing fertility to the deeper soil layers further
524 highlights how differences in biocrust type, element, soil depth, seasonality, and water inputs can

525 change the degree of connectivity between biocrusts and deeper soils. This study adds to our
526 understandings of how different biocrust types and deeper mineral soil exchange fertility and
527 provides nuance to the outcomes of nutrients and C cycling along successional gradients in
528 dryland regions. Future studies manipulating multiple abiotic variables, such as soil texture and
529 precipitation amounts, would further our understanding of connectivity and allow for improved
530 predictions of large scale biocrust contributions to the mineral soil.

531
532 **Acknowledgements**

533
534 Thanks to Peter Chuckran for feedback on analysis methods, Armin Howell for help designing
535 the leachate sample collection infrastructure, Suzanne Kosina for help with metabolite methods,
536 and Hilda Smith and Erika Geiger for support with experimental measurements. KEY and AD
537 were supported by National Science Foundation DEB #1557162 & #1557135. SF was supported
538 by USDA-NIFA-AFRI #2019-67020-29320 and National Science Foundation RII Track-2 FEC
539 #1826835. SCR and RR were supported by the Department of Defense (RC18-1322), the Joint
540 Fire Science Program (17-1-04-17), and the U.S. Geological Survey Ecosystems Mission area.
541 TN, TS, and SK were funded by the Office of Science Early Career Research Program, Office of
542 Biological and Environmental Research, of the U. S. Department of Energy under contract
543 number DE-AC02-05CH11231 to Lawrence Berkeley National Laboratory. Any use of trade,
544 firm, or product names is for descriptive purposes only and does not imply endorsement by the
545 U.S. Government.

546
547 **References**

548
549 Arbizu, P.M., 2017. pairwiseAdonis: Pairwise Multilevel Comparison using Adonis.
550 Austin, A.T., 2011. Has water limited our imagination for aridland biogeochemistry ? Trends

551 Ecol. Evol. 26, 229–235. doi:10.1016/j.tree.2011.02.003

552 Bao, T., Zhao, Y., Gao, L., Yang, Q., Yang, K., 2019. Moss-dominated biocrusts improve the
553 structural diversity of underlying soil microbial communities by increasing soil stability and
554 fertility in the Loess Plateau region of China. *Eur. J. Soil Biol.* 95, 103120.
555 doi:10.1016/j.ejsobi.2019.103120

556 Baran, R., Brodie, E.L., Mayberry-Lewis, J., Hummel, E., Da Rocha, U.N., Chakraborty, R.,
557 Bowen, B.P., Karaoz, U., Cadillo-Quiroz, H., Garcia-Pichel, F., Northen, T.R., 2015.
558 Exometabolite niche partitioning among sympatric soil bacteria. *Nat Commun* 6.

559 Barger, N.N., Belnap, J., Ojima, D.S., Mosier, A., 2005. NO gas loss from biologically crusted
560 soils in Canyonlands National Park, Utah. *Biogeochemistry* 75, 373–391.
561 doi:10.1007/s10533-005-1378-9

562 Barger, N.N., Castle, S.C., Dean, G.N., 2013. Denitrification from nitrogen-fixing biologically
563 crusted soils in a cool desert environment, southeast Utah, USA. *Ecol. Process.* 2, 1.
564 doi:10.1186/2192-1709-2-16

565 Barger, N.N., Weber, B., Garcia-Pichel, F., Zaady, E., Belnap, J., 2016. Patterns and Controls on
566 Nitrogen Cycling of Biological Soil Crusts, in: *Biological Soil Crusts: An Organizing*
567 *Principle in Drylands*. pp. 257–287.

568 Barr, D., 1999. Biotic and abiotic regulation of nitrogen dynamics in biological soil crusts.
569 Northern Arizona University, Flagstaff, AZ.

570 Beck, T., Joergensen, G., Kandeler, E., Makeschin, F., Nuss, E., Oberholzer, H.R., Scheu, S.,
571 1997. An inter-laboratory comparison of ten different ways of measuring soil microbial
572 biomass C. *Soil Biol. Biochem.* 29, 1023–1032. doi:10.2307/3898317

573 Belnap J. 2001. Factors Influencing Nitrogen Fixation and Nitrogen Release in Biological Soil

574 Crusts. In: Belnap J., Lange O.L. (eds) *Biological Soil Crusts: Structure, Function, and*
575 *Management. Ecological Studies (Analysis and Synthesis)*, vol 150. Springer, Berlin,
576 Heidelberg. https://doi.org/10.1007/978-3-642-56475-8_19

577 Belnap J., Eldridge D. 2001. Disturbance and Recovery of Biological Soil Crusts. In: Belnap J.,
578 Lange O.L. (eds) *Biological Soil Crusts: Structure, Function, and Management. Ecological*
579 *Studies (Analysis and Synthesis)*, vol 150. Springer, Berlin, Heidelberg.
580 https://doi.org/10.1007/978-3-642-56475-8_27

581 Belnap, J., O.L. Lange, O.L. 2001 *Biological Soil Crusts: Structure, Function, and Management.*
582 *Ecological Studies (Analysis and Synthesis)*, vol 150. Springer, Berlin, Heidelberg.
583 https://doi.org/10.1007/978-3-642-56475-8_27

584 Beraldi-Campesi, H., Hartnett, H.E., Anbar, A., Gordon, G.W., Garcia-Pichel, F., 2009. Effect of
585 biological soil crusts on soil elemental concentrations: Implications for biogeochemistry and
586 as traceable biosignatures of ancient life on land. *Geobiology* 7, 348–359.
587 [doi:10.1111/j.1472-4669.2009.00204.x](https://doi.org/10.1111/j.1472-4669.2009.00204.x)

588 Brankatschk, R., Fischer, T., Veste, M., Zeyer, J., 2013. Succession of N cycling processes in
589 biological soil crusts on a Central European inland dune. *FEMS Microbiol. Ecol.* 83, 149–
590 160. [doi:10.1111/j.1574-6941.2012.01459.x](https://doi.org/10.1111/j.1574-6941.2012.01459.x)

591 Brookes, P.C., Kragt, J.F., Powlson, D.S., Jenkinson, D.S., 1985. Chloroform fumigation and the
592 release of soil nitrogen: The effects of fumigation time and temperature. *Soil Biol.*
593 *Biochem.* 17, 831–835. [doi:10.1016/0038-0717\(85\)90143-9](https://doi.org/10.1016/0038-0717(85)90143-9)

594 Castle, S.C., Morrison, C.D., Barger, N.N., 2011. Extraction of chlorophyll *a* from biological soil
595 crusts: A comparison of solvents for spectrophotometric determination. *Soil Biol. Biochem.*
596 43, 853–856. [doi:10.1016/j.soilbio.2010.11.025](https://doi.org/10.1016/j.soilbio.2010.11.025)

597 Chamizo, Sonia, Cantón, Y., Miralles, I., Domingo, F., 2012. Biological soil crust development
598 affects physicochemical characteristics of soil surface in semiarid ecosystems. *Soil Biol.*
599 *Biochem.* 49, 96–105. doi:10.1016/j.soilbio.2012.02.017

600 Chaudhary, V.B., Bowker, M.A., Dell, T.E.O., Grace, J.B., Redman, E., Rillig, M.C., Johnson,
601 N.C., 2009. Untangling the Biological Contributions to Soil Stability in Semiarid
602 Shrublands Published by : Ecological Society of America content in a trusted digital archive
603 . We use information technology and tools to increase productivity and facilitate new forms.
604 *Ecol. Appl.* 19, 110–122.

605 Cleveland, C.C., Nemergut, D.R., Schmidt, S.K., Alan, R., Schmidt, S.K., Townsend, A.R.,
606 2006. Increases in Soil Respiration following Labile Carbon Additions Linked to Rapid
607 Shifts in Soil Microbial Community Composition Linked references are available on
608 JSTOR for this article : Increases in soil respiration following labile carbon additions link.
609 *Biogeochemistry* 82, 229–240. doi:10.1007/s10533-006-9065-z

610 Cleveland, C.C., Wieder, W.R., Reed, S.C., Townsend, A.R., 2010. Experimental drought in a
611 tropical rain forest increases soil carbon dioxide losses to the atmosphere. *Ecology* 91,
612 2313–2323. doi:10.1890/09-1582.1

613 Colesie, C., Felde, V.J.M.N.L., Budel, B., 2016. Composition and Macrostructure of Biological
614 Soil Crusts, in: Weber, B., Budel, B., Belnap, J. (Eds.), *Biological Soil Crusts: An*
615 *Organizing Principle in Drylands*. Springer International Publishing, pp. 159–172.

616 Collins, S., Belnap, J., Grimm, N., Rudgers, J., Dahm, C., D’Odoric, D., Litvak, M., Natvig, D.,
617 Peters, D., Pockman, W., Sinsabaugh, R., Wolf, B., 2014. A multi-scale hierarchical model
618 of pulse dynamics in aridland ecosystems. *Annu. Rev. Ecol. Evol. Syst.* 45, 397–419.

619 Couradeau, E., Giraldo-Silva, A., De Martini, F., Garcia-Pichel, F., 2019. Spatial segregation of

620 the biological soil crust microbiome around its foundational cyanobacterium, *Microcoleus*
621 *vaginatus*, and the formation of a nitrogen-fixing cyanosphere. *Microbiome* 7, 1–12.
622 doi:10.1186/s40168-019-0661-2

623 Couradeau, E., Karaoz, U., Lim, H.C., Nunes da Rocha, U., Northen, T., Brodie, E., Garcia-
624 Pichel, F., 2016. Bacteria increase arid-land soil surface temperature through the production
625 of sunscreens. *Nat. Commun.* 7, 10373. doi:10.1038/ncomms10373

626 Darrouzet-Nardi, A., 2020. *treateffect*: Calculates and plots treatment effect sizes from
627 experiments.

628 Darrouzet-Nardi, A., Reed, S.C., Grote, E.E., Belnap, J., 2015. Observations of net soil exchange
629 of CO₂ in a dryland show experimental warming increases carbon losses in biocrust soils.
630 *Biogeochemistry* 126, 363–378. doi:10.1007/s10533-015-0163-7

631 Davies, B.E., 1974. Loss-on-Ignition as an Estimate of Soil Organic Matter¹. *Soil Sci. Soc. Am.*
632 *J.* 38, 150. doi:10.2136/sssaj1974.03615995003800010046x

633 Delgado-Baquerizo, M., Covelo, F., Maestre, F.T., Gallardo, A., 2013. Biological soil crusts
634 affect small-scale spatial patterns of inorganic N in a semiarid Mediterranean grassland. *J.*
635 *Arid Environ.* 91, 147–150. doi:10.1016/j.jaridenv.2013.01.005

636 Delgado-Baquerizo, M., Maestre, F.T., Eldridge, D.J., Bowker, M.A., Ochoa, V., Gozalo, B.,
637 Berdugo, M., Val, J., Singh, B.K., 2015. Biocrust-forming mosses mitigate the negative
638 impacts of increasing aridity on ecosystem multifunctionality in drylands. *New Phytol.*
639 doi:10.1111/nph.13688

640 Dümig, A., Veste, M., Hagedorn, F., Fischer, T., Lange, P., Spröte, R., Kögel-Knabner, I., 2013.
641 Biological soil crusts on initial soils: organic carbon dynamics and chemistry under
642 temperate climatic conditions. *Biogeosciences Discuss.* 10, 851–894. doi:10.5194/bgd-10-

643 851-2013

644 Ferrenberg, S., Faist, A.M., Howell, A., Reed, S.C., 2018a. Biocrusts enhance soil fertility and
645 *Bromus tectorum* growth, and interact with warming to influence germination. *Plant Soil*
646 429, 77–90. doi:10.1007/s11104-017-3525-1

647 Ferrenberg, S., Reed, S.C., Belnap, J., 2015. Climate change and physical disturbance cause
648 similar community shifts in biological soil crusts. *Proc. Natl. Acad. Sci.* 112, 12116–12121.
649 doi:10.1073/pnas.1509150112

650 Garcia-Pichel, F., Belnap, J., 1996. Microenvironments and microscale productivity of
651 cyanobacterial desert crusts. *J. Phycol.* 32, 774–782. doi:10.1111/j.0022-3646.1996.00774.x

652 Garcia-Pichel, F., López-Cortés, A., Nübel, U., 2001. Phylogenetic and Morphological Diversity
653 of Cyanobacteria in Soil Desert Crusts from the Colorado Plateau. *Appl. Environ.*
654 *Microbiol.* 67, 1902–1910. doi:10.1128/AEM.67.4.1902-1910.2001

655 Garcia-Pichel, F., Loza, V., Marusenko, Y., Mateo, P. and Potrafka, R.M., 2013. Temperature
656 drives the continental-scale distribution of key microbes in topsoil
657 communities. *Science.* 340:6140. 1574-1577.

658 Guo, Y., Zhao, H., Zuo, X., Drake, S., Zhao, X., 2008. Biological soil crust development and its
659 topsoil properties in the process of dune stabilization, Inner Mongolia, China. *Environ.*
660 *Geol.* 54, 653–662. doi:10.1007/s00254-007-1130-y

661 Hart, S.C., Stark, J.M., Davidson, E.A., Firestone, M.K., 1994. Nitrogen Mineralization,
662 Immobilization, and Nitrification, in: *Methods of Soil Analysis: Part 2 Microbiological and*
663 *Biochemical Properties 5.* John Wiley & Sons, Ltd, pp. 985–1018.
664 doi:10.2136/sssabookser5.2.c42

665 Hartley, A., Barger, N., Belnap, J., Okin, G., 2007. Dryland Ecosystems, in: Marschner, P.,

666 Rengel, Z. (Eds.), *Nutrient Cycling in Terrestrial Ecosystems*. Springer-Verlag, Berlin
667 Heidelberg, pp. 271–299.

668 Housman, D.C., Powers, H.H., Collins, A.D., Belnap, J., 2006. Carbon and nitrogen fixation
669 differ between successional stages of biological soil crusts in the Colorado Plateau and
670 Chihuahuan Desert. *J. Arid Environ.* 66, 620–634. doi:10.1016/j.jaridenv.2005.11.014

671 Johnson, S.L., Budinoff, C.R., Belnap, J., Garcia-Pichel, F., 2005. Relevance of ammonium
672 oxidation within biological soil crust communities. *Environ. Microbiol.* 7, 1–12.
673 doi:10.1111/j.1462-2920.2004.00649.x

674 Kuo, S., 1996. Phosphorus, in: Sparks, D.L. (Ed.), *Methods of Soil Analysis*. Soil Science
675 Society of America Book Series, No. 5, Soil Science of America, Madison, WI, USA, pp.
676 869–919.

677 Maestre, F.T., Escolar, C., de Guevara, M.L., Quero, J.L., Lázaro, R., Delgado-Baquerizo, M.,
678 Ochoa, V., Berdugo, M., Gozalo, B., Gallardo, A., 2013. Changes in biocrust cover drive
679 carbon cycle responses to climate change in drylands. *Glob. Chang. Biol.* 19, 3835–3847.
680 doi:10.1111/gcb.12306

681 Mayland, H.F., McIntosh, T.H., 1966. Distribution of Nitrogen Fixed in Desert Algal-Crusts.
682 *Soil Sci. Soc. Am. J.* 30, 606–609. doi:10.2136/sssaj1966.03615995003000050021x

683 Miralles, I., Domingo, F., García-Campos, E., Trasar-Cepeda, C., Leirós, M.C., Gil-Sotres, F.,
684 2012. Biological and microbial activity in biological soil crusts from the Tabernas desert, a
685 sub-arid zone in SE Spain. *Soil Biol. Biochem.* 55, 113–121.
686 doi:10.1016/j.soilbio.2012.06.017

687 Moreira-Grez, B., Tam, K., Cross, A.T., Yong, J.W.H., Kumaresan, D., Nevill, P., Farrell, M.,
688 Whiteley, A.S., 2019. The Bacterial Microbiome Associated With Arid Biocrusts and the

689 Biogeochemical Influence of Biocrusts Upon the Underlying Soil. *Front. Microbiol.* 10, 1–
690 22. doi:10.3389/fmicb.2019.02143

691 Nelson C, Giraldo-Silva A, Garcia-Pichel F (2021) A symbiotic nutrient exchange within the
692 cyanosphere microbiome of the biocrust cyanobacterium, *Microcoleus vaginatus*. *ISME J*
693 15:282–292. <https://doi.org/10.1038/s41396-020-00781-1>

694 Oksanen, J., Blanchet, F.G., Friendly, M., Kindt, R., Legendre, P., McGlenn, D., Minchin, P.,
695 O’Hara, R., Simpson, G., Solymos, P., Henry, M., Stevens, H., Szoecs, E., Wagner, H.,
696 2019. *vegan: Community Ecology Package*.

697 Olsen, S., 1954. Estimation of available phosphorus in soils by extraction with sodium
698 bicarbonate. *USDA Circ.* 1–19.

699 Porada, P., Weber, B., Elbert, W., Pöschl, U., Kleidon, A., 2014. Estimating impacts of lichens
700 and bryophytes on global biogeochemical cycles 71–85.
701 doi:10.1002/2013GB004705.Received

702 Qiu, S., McComb, A.J., Bell, R.W., Davis, J.A., 2005. Response of soil microbial activity to
703 temperature, moisture, and litter leaching on a wetland transect during seasonal refilling.
704 *Wetl. Ecol. Manag.* 13, 43–54. doi:10.1007/s11273-003-3054-y

705 Reed, S.C., Coe, K.K., Sparks, J.P., Housman, D.C., Zelikova, T.J., Belnap, J., 2012. Changes to
706 dryland rainfall result in rapid moss mortality and altered soil fertility. *Nat. Clim. Chang.* 2,
707 752–755. doi:10.1038/NCLIMATE1596

708 Reed, S.C., Maestre, F.T., Ochoa-Hueso, R., Kuske, C.R., Darrouzet-Nardi, A., Oliver, M.,
709 Darby, B., Sancho, L.G., Sinsabaugh, R.L., Belnap, J., 2016. Biocrusts in the Context of
710 Global Change, in: Weber B., Büdel B., Belnap J. (Eds.), *Biological Soil Crusts: An*
711 *Organizing Principle in Drylands*. Springer, Cham, pp. 451–476. doi:10.1007/978-3-319-

712 30214-0_22

713 Ritchie, R.J., 2008. Universal chlorophyll equations for estimating chlorophylls a, b, c, and d and
714 total chlorophylls in natural assemblages of photosynthetic organisms using acetone,
715 methanol, or ethanol solvents. *Photosynthetica* 46, 115–126. doi:10.1007/s11099-008-0019-
716 7

717 Robertson, G.P., Wedin, D., Groffman, P.M., Blair, J.M., Holland, E.M., Nadelhoffer, K.J.,
718 Harris, D., 1999. Soil carbon and nitrogen availability: nitrogen mineralization and soil
719 respiration potentials, in: Robertson, G.P., Coleman, D.C., Bledsoe, C.S., Sollins, P. (Eds.),
720 *Standard Methods of Long-Term Ecological Research*. Oxford University Press, New York,
721 New York, USA, pp. 258–271.

722 Rosentreter R., Belnap J. (2001) Biological Soil Crusts of North America. In: Belnap J., Lange
723 O.L. (eds) *Biological Soil Crusts: Structure, Function, and Management*. Ecological Studies
724 (Analysis and Synthesis), vol 150. Springer, Berlin, Heidelberg.
725 https://doi.org/10.1007/978-3-642-56475-8_2

726 Rossi, F., Mugnai, G., De Philippis, R., 2018. Complex role of the polymeric matrix in biological
727 soil crusts. *Plant Soil* 429, 19–34. doi:10.1007/s11104-017-3441-4

728 Rudgers, J.A., Dettweiler-Robinson, E., Belnap, J., Green, L.E., Sinsabaugh, R.L., Young, K.E.,
729 Cort, C.E., Darrouzet-Nardi, A., 2018. Are fungal networks key to dryland primary
730 production? *Am. J. Bot.* 105, 1783–1787. doi:10.1002/ajb2.1184

731 Sancho, L.G., Belnap, J., Colesie, C., Raggio, J., Weber, B, 2016. Carbon Budgets of Biological
732 Soil Crusts at Micro-, Meso-, and Global Scales, in: Weber, Bettina, Budel, B., Belnap, J.
733 (Eds.), *Biological Soil Crusts: An Organizing Principle in Drylands*. Springer International
734 Publishing, pp. 287–304.

735 Soil Survey Staff, Natural Resources Conservation Service, United States Department of
736 Agriculture. Web Soil Survey. Available online at the following
737 link: <http://websoilsurvey.sc.egov.usda.gov/>.

738 Sparks, D.L., Page, A.L., Helmke, P.A., Loeppert, R.H. (Eds.), 1996. *Methods of Soil Analysis*
739 *Part 3—Chemical Methods*, 5.3. ed, SSSA Book Series. Soil Science Society of America,
740 American Society of Agronomy, Madison, WI. doi:10.2136/sssabookser5.3.frontmatter

741 Steppe, T.F., Olson, J.B., Paerl, H.W., Litaker, R.W., Belnap, J., 1996. Consortial N₂ fixation: A
742 strategy for meeting nitrogen requirements of marine and terrestrial cyanobacterial mats.
743 *FEMS Microbiol. Ecol.* 21, 149–156. doi:10.1016/S0168-6496(96)00047-5

744 Steven, B., Gallegos-Graves, L.V., Belnap, J., Kuske, C.R., 2013. Dryland soil microbial
745 communities display spatial biogeographic patterns associated with soil depth and soil
746 parent material. *FEMS Microbiol. Ecol.* 86, 101–113. doi:10.1111/1574-6941.12143

747 Stewart, W.D.P., 1967. Transfer of biologically fixed nitrogen in a sand dune slack region [18].
748 *Nature*. doi:10.1038/214603a0

749 Swenson, T.L., Couradeau, E., Bowen, B.P., De Philippis, R., Rossi, F., Mugnai, G., Northen,
750 T.R., 2018. A novel method to evaluate nutrient retention by biological soil crust
751 exopolymeric matrix. *Plant Soil* 429, 53–64. doi:10.1007/s11104-017-3537-x

752 Swenson, T.L., Jenkins, S., Bowen, B.P., Northen, T.R., 2015. Untargeted soil metabolomics
753 methods for analysis of extractable organic matter. *Soil Biol. Biochem.* 80, 189–198.
754 doi:10.1016/j.soilbio.2014.10.007

755 Thomazo, C., Couradeau, E., Garcia-Pichel, F., 2018. Possible nitrogen fertilization of the early
756 Earth Ocean by microbial continental ecosystems. *Nat. Commun.* 9. doi:10.1038/s41467-
757 018-04995-y

758 Torres-Cruz, T.J., Howell, A.J., Reibold, R.H., McHugh, T.A., Eickhoff, M.A., Reed, S.C.,
759 2018. Species-specific nitrogenase activity in lichen-dominated biological soil crusts from
760 the Colorado Plateau, USA. *Plant Soil*. doi:10.1007/s11104-018-3580-2

761 Tucker, C.L., Ferrenberg, S. and Reed, S.C., 2019. Climatic sensitivity of dryland soil CO₂
762 fluxes differs dramatically with biological soil crust successional state. *Ecosystems*, 22,
763 15-32. <https://doi.org/10.1007/s10021-018-0250-4>

764 Tucker, C., Ferrenberg, S., Reed, S.C., 2020. Modest Residual Effects of Short-Term Warming,
765 Altered Hydration, and Biocrust Successional State on Dryland Soil Heterotrophic Carbon
766 and Nitrogen Cycling. *Front. Ecol. Evol.* 8, 1–17. doi:10.3389/fevo.2020.467157

767 Weber, B., Bowker, M.A., Zhang, Y., Belnap, J., 2016. Natural Recovery of Biological Soil
768 Crusts After Disturbance, in: *Biological Soil Crusts: An Organizing Principle in Drylands*.
769 pp. 479–498.

770 Weintraub, M.N., Scott-Denton, L.E., Schmidt, S.K., Monson, R.K., 2007. The effects of tree
771 rhizodeposition on soil exoenzyme activity, dissolved organic carbon, and nutrient
772 availability in a subalpine forest ecosystem. *Oecologia* 154. doi:doi:10.1007/s00442-007-
773 0804-1

774 Wertin, T.M., Phillips, S.L., Reed, S.C. Belnap, J., 2012. Elevated CO₂ did not mitigate the
775 effect of a short-term drought on biological soil crusts. *Biology and Fertility of Soils*, 48,
776 797-805.

777 Yang, X., Xu, M., Zhao, Y., Gao, L., Wang, S., 2019. Moss-dominated biological soil crusts
778 improve stability of soil organic carbon on the loess plateau, China. *Plant, Soil Environ.* 65,
779 104–109. doi:10.17221/473/2018-PSE

780 Zelikova, T.J., Housman, D.C., Grote, E.E., Neher, D.A., Belnap, J., 2012. Warming and

781 increased precipitation frequency on the Colorado Plateau: Implications for biological soil
782 crusts and soil processes. *Plant Soil*. doi:10.1007/s11104-011-1097-z

783 Zhao, Y., Zhang, Z., Hu, Y., Chen, Y., 2016. The seasonal and successional variations of carbon
784 release from biological soil crust-covered soil. *J. Arid Environ.* 127, 148–153.
785 doi:10.1016/j.jaridenv.2015.11.012

786 Zho, X., Tu, W., 1999. Comparison of Several Independent Population Means When Their
787 Samples Contain Log- Normal and Possibly Zero Observations. *Biometrics* 55, 645–651.

788 Zhou, X.H., Tu, W., 2000. Interval estimation for the ration in means of log-normally distributed
789 medical costs with zero values. *Comput. Stat. Data Anal.* 35, 201–210.

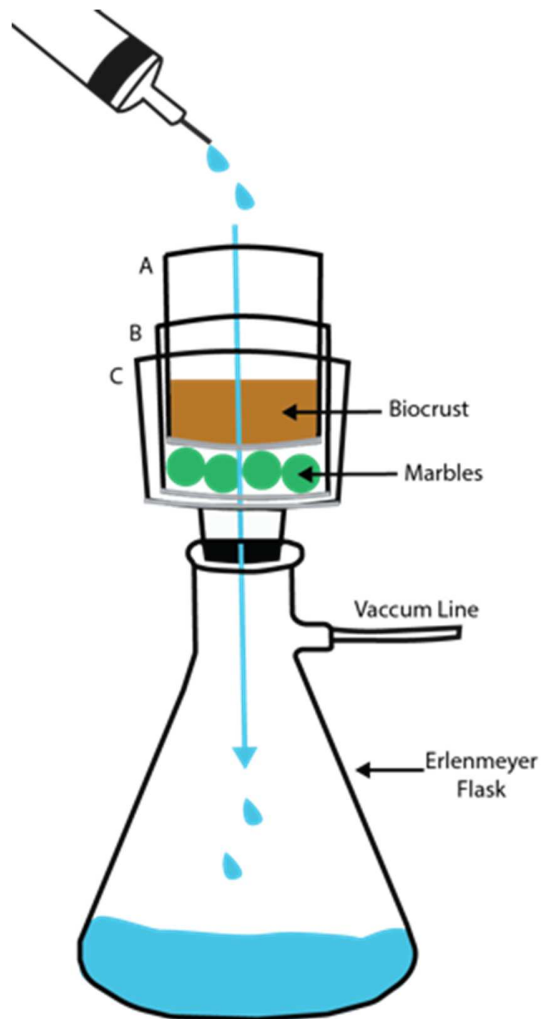
790

791

792

793

794 **Figures**
795



796
797

798 Figure 1. The collection system used to collect leachate from biocrusts. Biocrusts were placed in
799 a plastic cylinder (A), that was open on the top with a 1.18 mm mesh screen (shown in grey) at
800 the bottom. Cylinder A was placed within a second plastic cylinder (B) open on the top and with
801 a layer of marbles resting on a mesh screen (shown in grey). Marbles were used to ensure
802 sediment did not pool over the filter. Cylinders A and B were placed in a Buchner funnel (C)
803 with a 55 mm Whatman #1 filter on the bottom (show in grey). Watering treatments were
804 administered across the biocrust using a syringe. Water moved through cylinders A and B and

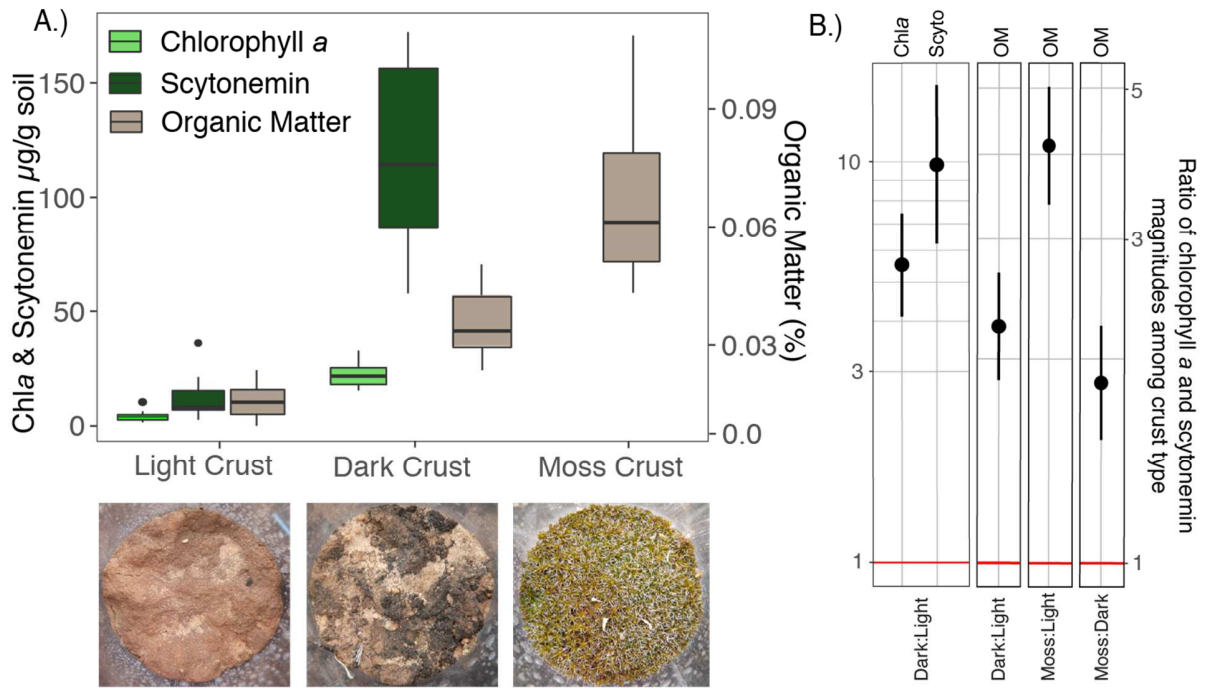
805 through the funnel and filter into an Erlenmeyer flask. Water was pulled through the system

806 using vacuum filtration and immediately collected and frozen until analysis.

807

808

809



810

811 Figure 2. A.) The amount of chlorophyll *a* and scytonemin in μg per g of soil in lightly
 812 pigmented and darkly pigmented cyanobacterial crusts and the percent organic matter in all three
 813 biocrust types pictured in the figure (chlorophyll *a* and scytonemin were not measured in moss
 814 dominated crusts). Vertical bars on the boxplots represent median values and the vertical lines
 815 represent minimum and maximum values. B.) Ratios with 95 % confidence intervals among
 816 biocrust successional stage comparing chlorophyll *a*, scytonemin, and organic matter
 817 concentration. Confidence intervals not crossing 1 would be considered statistically significant.

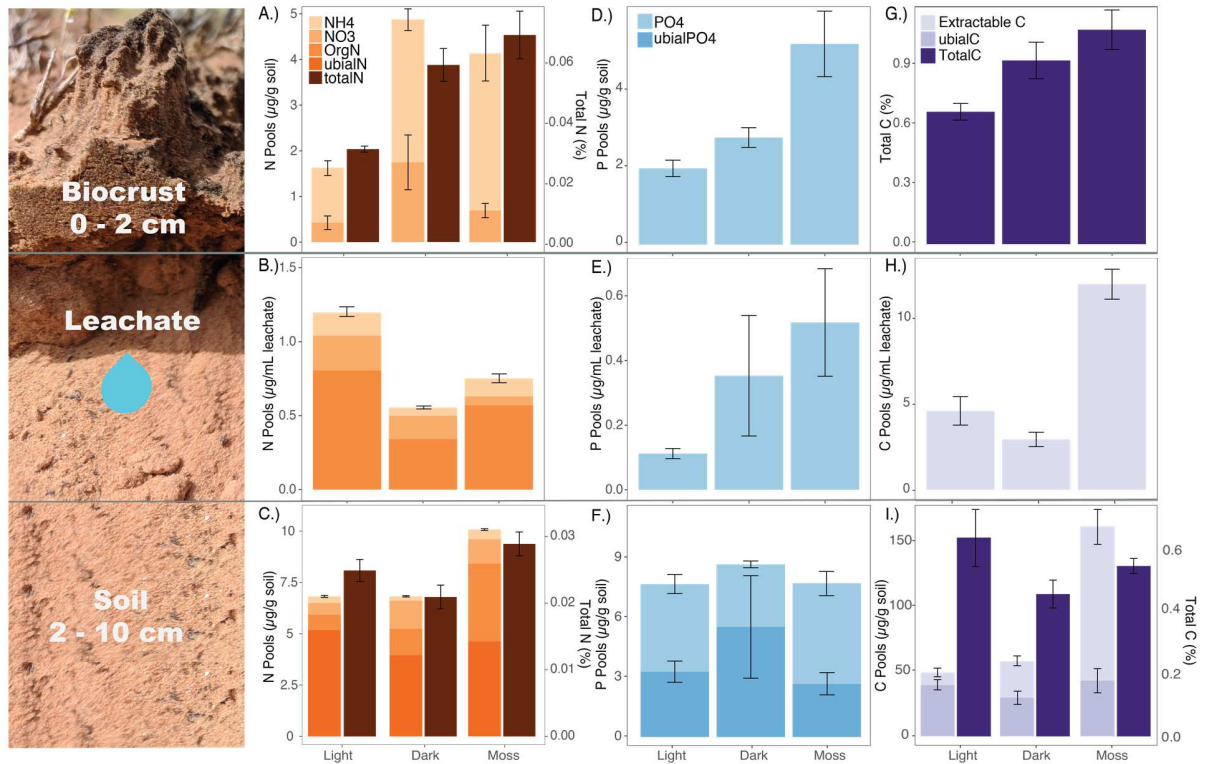
818

819

820

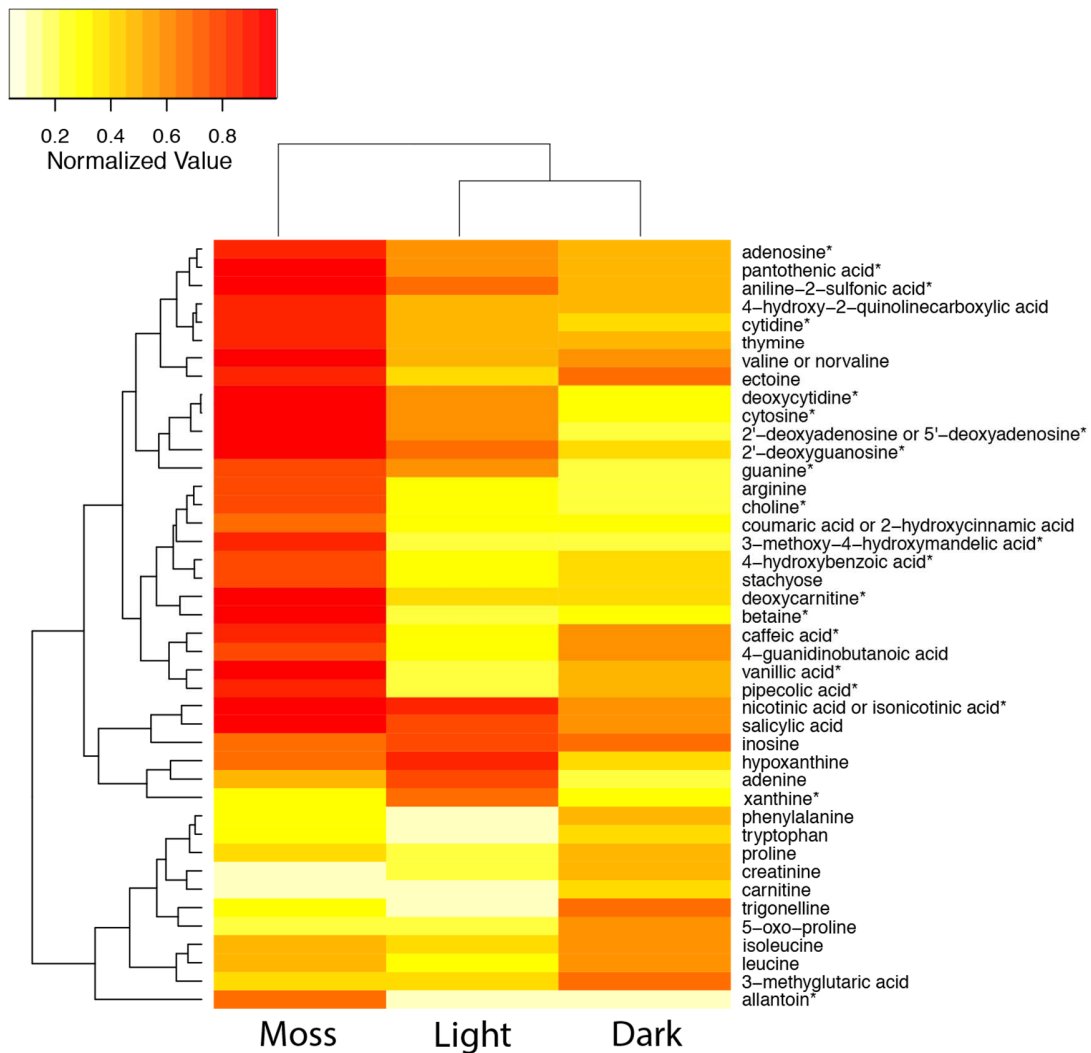
821

822



823
 824
 825
 826
 827
 828
 829
 830
 831
 832
 833
 834
 835

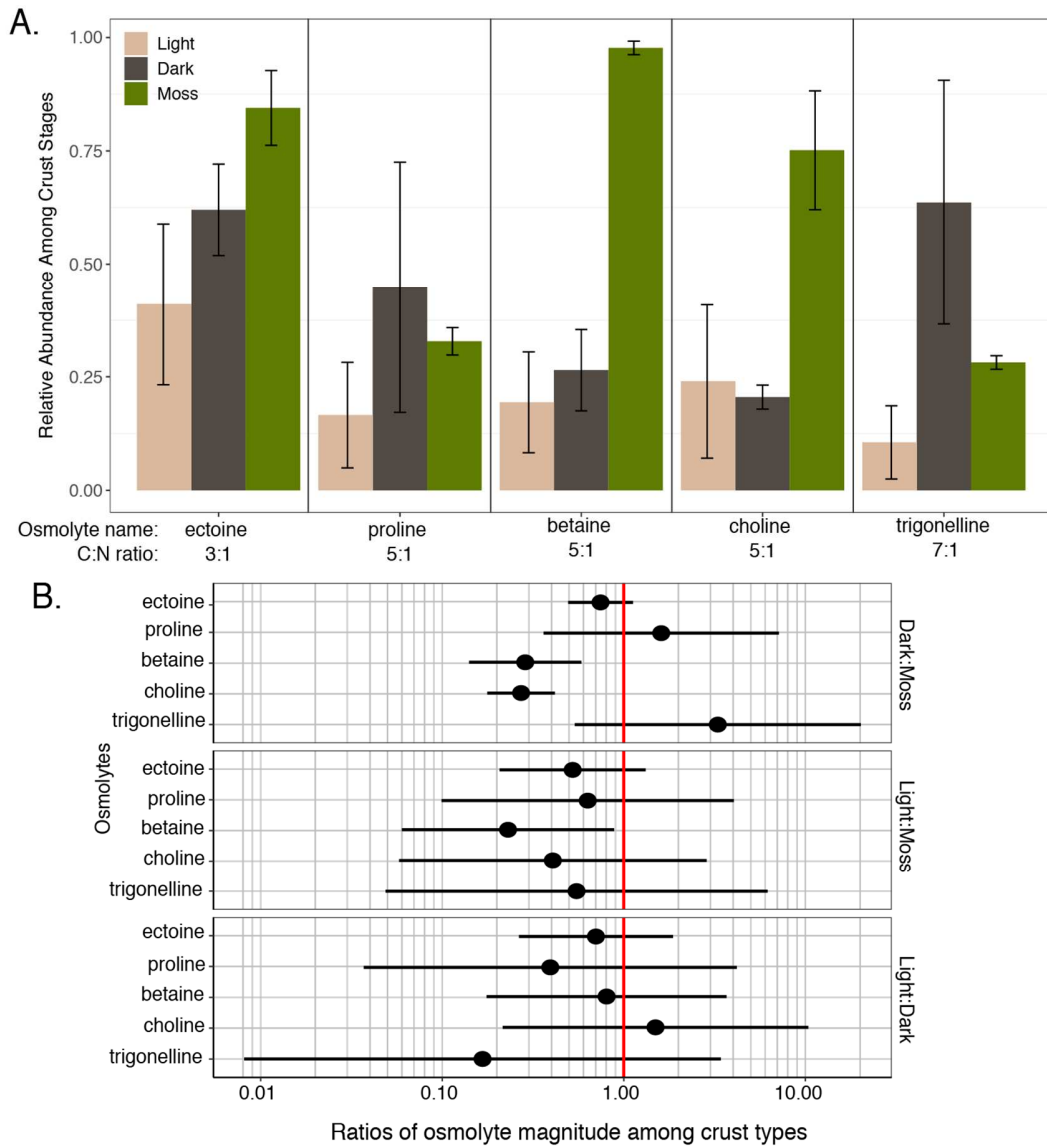
Figure 3. Top row: Nutrient and C concentrations in field collected biocrust (0-2 cm) (A., D., G.), middle row: nutrient and C concentrations released in leachate (B., E., H.) and bottom row: nutrient and C concentrations in the field collected soil directly beneath biocrust (2-10 cm) (C., F., I.). In the leachate layer, N, P, and C values are summed across the four time points of the experiment. Error bars represent SE. Overlapping error bars were removed to reduce confusion and are listed as follows: B). NO_3^- : light SE \pm 0.022, dark SE \pm 0.023 moss SE \pm 0.018, TDN: light SE \pm 0.14, dark SE \pm 0.06, moss SE \pm 0.07 C). NO_3^- : light SE \pm 0.19, dark SE \pm 0.27, moss SE \pm 0.14, TDN: light SE \pm 0.16, dark SE \pm 0.14, moss SE \pm 0.48, microbial N: light SE \pm 0.54, dark SE \pm 0.62, moss SE \pm 0.96).



836
837
838

839 Figure 4. Comparison of relative intensity of detected metabolites from the three biocrust
840 successional stages: moss dominated crust (Moss), lightly pigmented cyanobacterial crust
841 (Light), and darkly pigmented cyanobacterial crust (Dark). Peak values were normalized to the
842 largest peak value for each metabolite across biocrust successional stages. 0 indicates the lowest
843 relative abundance and 1 represents the highest relative abundance. The dendrogram on the left
844 and top clusters similarly extracted metabolites based on hierarchical clustering and the heat map
845 displays the intensity of metabolites normalized to the most intense peak within each row

846 (metabolite). * indicates metabolite intensities that are statistically different (based on an alpha
847 level of 0.05) among the three biocrust types. Only confirmed metabolites were included.
848



850

851

852

Figure 5: A. The normalized abundance among biocrust types of common, confirmed osmolytes

853

found within the leachate in order of increasing C:N ratio. While comparisons across osmolyte

854

types cannot be made, the order of magnitude of the average peak area across biocrust

855

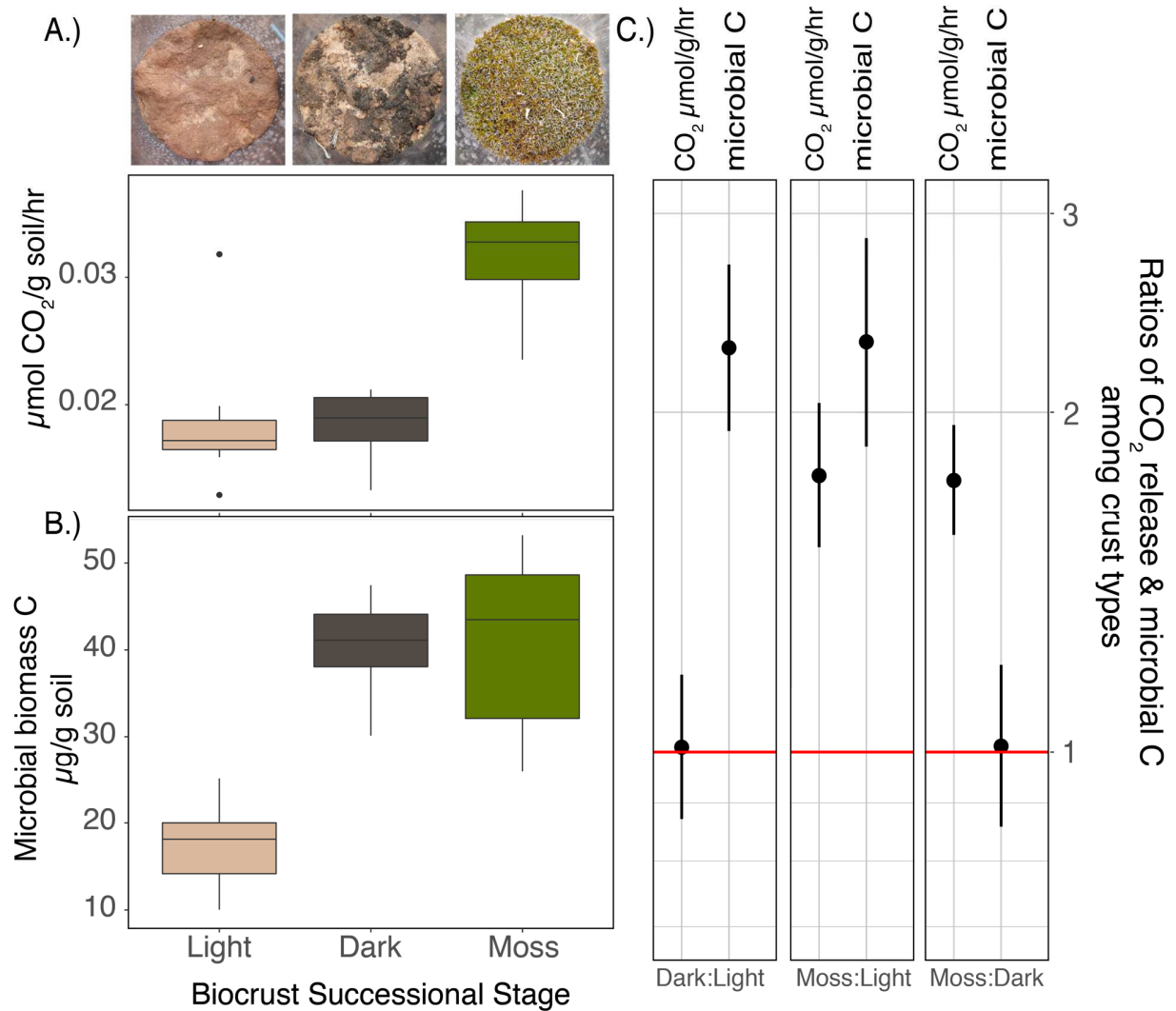
successional stages for each osmolyte is included to show potential differences in the quantity of

856

the different osmolytes. B. Ratios with 95 % confidence intervals among biocrust successional

857 stages for each osmolyte. Confidence intervals not containing 1 would be considered statistically
858 significant.

859



860
861

862 Figure 6. A). Respiration rates ($\mu\text{mol CO}_2/\text{g dry soil/hr}$) of soils collected from beneath the three
863 biocrust successional states during a 24 hr incubation B). Changes to microbial biomass C
864 concentrations within mineral soil collected from beneath the three different biocrust
865 successional states after a 24 hr incubation. Vertical bars on the boxplots represent median
866 values and the vertical lines represent minimum and maximum values. C). Ratios with 95 %
867 confidence intervals among biocrust successional stages for soil CO_2 respiration ($\text{CO}_2 \mu\text{mol/g/hr}$)
868 and microbial biomass C. Confidence intervals not crossing 1 would be considered statistically
869 significant.